



*Dedicated to Professor Alexandru T. Balaban
on the occasion of his 80th anniversary*

CIRCULAR DICHROISM CHARACTERISATION OF THE INCLUSION COMPLEXES OF 2-ACETYL-PHENOXATHIIN SULPHONE WITH CYCLODEXTRINS: EXPERIMENTAL DATA AND TDDFT CALCULATIONS

Romică SANDU^a and Mihaela HILLEBRAND^{b*}

^a Institute of Physical Chemistry, "Ilie Murgulescu" Roumanian Academy, Splaiul Independentei 202, Bucharest 060021, Roumania

^b Department Physical Chemistry, Fac. of Chemistry, University of Bucharest, Bd. Regina Elisabeta 4-12, Bucharest, Roumania

Received December 20, 2010

The Induced Circular Dichroism spectra of the inclusion complexes of a phenoxathiin derivative, 2-acetylphenoxathiin-sulphone, with three cyclodextrins (CyD), α -, β - and 2-HP- β -CyD, differing by the dimension of the cavity are reported and discussed. The experimental data were used for the estimation of the association constants and 1:1 stoichiometry for β - and 2-HP- β -CyD, and, secondly, for getting an insight on the inclusion mode of the ligand in the cavity. The correlation of the ligand orientation in the cavity as predicted by the rules of Harata and Kodaka from the signs of the experimental dichroic signals with the results of TDDFT calculations on the energies, oscillatory strengths and polarizations of the electronic transition, shows that the ligand is included with the long molecular axis parallel to the cavity axis in β - and 2-HP- β -CyD, and in an orthogonal position in α -CyD, leading presumably to the formation of a 1:2 ligand: CyD complex. The calculations allow for the explanation of the differences in the circular dichroism spectra in β - and 2-HP- β -CyD on the basis of the preferential inclusion of different conformers depending on the cavity dimension.

INTRODUCTION

The experimental study of the inclusion complexes of cyclodextrins (CyDs) with different organic compounds was widely performed, due to the frequent applications in the pharmaceutical chemistry.¹⁻⁴ The possibility to enhance the solubility of several drugs by their inclusion in the CyD cavity and the remarkable physical and chemical properties of the inclusion complexes determine a continuously increasing interest in this field manifested in the publication of several books and reviews.⁵⁻⁸ The main aspects considered were the stoichiometry of the complexes, the association constants, the thermodynamic parameters and the conformational changes due to the restricted internal motions.⁹⁻¹³ Few papers dealt with the

experimental determination of the structural aspects, the method that can provide such information in solutions being the bidimensional NMR spectroscopy.^{14,15} However, it was found that the circular dichroism spectroscopy could also provide such information, even in the case of achiral ligands. The inclusion of the ligand in the chiral cavity of the CyD determines a molecular asymmetry reflected in the appearance of an induced circular dichroic (ICD) signal characterized by its position, intensity and sign.¹⁶⁻²⁶ The position of the ICD band corresponds to the position of the electronic absorption band of the chromophore and the intensity depends on the asymmetry factor g , defined as the ratio of the difference in the absorptivity in circularly left and right polarised light and the absorptivity in

* Correspondent author: mihaela.hillebrand@gmail.com

isotropic light, $g = \Delta\epsilon / \epsilon$. The sign of the dichroic signal is correlated with the relative position of the transition moment of the electronic band and the axis of the CyD cavity. According to the semiempirical Harata-Kodaka rules,²⁷⁻³² if the transition moment is parallel to the cavity axis, the dichroic signal is positive, while if the transition moment is directed orthogonal to the cavity axis, the sign is negative. The correlation of the experimental data with TDDFT calculations on the energies and polarization of the electronic transitions allows for a better understanding of the structural aspects of the inclusion process.

The aim of this paper is to characterize by circular dichroism spectroscopy the inclusion complexes of a phenoxathiin derivative, 2-acetylphenoxathiin-sulphone (**I**, Fig. 1) with three CyDs, α -, β - and 2-HP- β -CyD, differing by the dimension of the cavity. The results of TDDFT calculations will be used to rationalize the experimental ICD spectral data. We will mainly focus on the possibility to use the experimental CD data for obtaining starting reliable structures for further optimization on the supramolecular CyD-ligand systems.

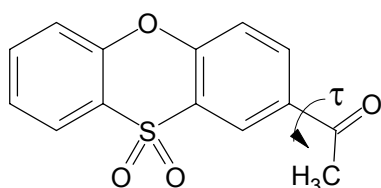


Fig. 1 – Structure of the ligand, 2-acetylphenoxathiin-sulphone (**I**). τ represents the torsion angle of the acetyl group in respect to the heteroring.

EXPERIMENTAL AND CALCULATION METHODS

The inclusion complexes were prepared by adding to a stock solution (10^{-5} M in methanol:water 1:9, v:v) of the title compound, aliquots of the CyD solutions (10^{-2} M) maintaining in all the samples the same concentration of ligand.

The ICD spectra were recorded at room temperature on a Jasco J-815 CD spectrometer using a 1.00 cm cell at 0.2 nm intervals, with three scans averaged for each CD spectrum in the range 200–400 nm; the results are expressed as ellipticity (θ) in millidegrees (mdeg).

The MO calculations were performed by DFT and TDDFT methods using the Gaussian03 program,³³ considering different possible conformers characterized by the dihedral angle τ (Fig.1), describing the position of the acetyl group in respect to the heteroring. Two functionals, B3LYP³⁴ and PBE^{35,36} were used in conjunction with the 6-31G basis set.³⁷

The optimisations were performed considering the solvent, water, in the frame of the Polarizable Continuum Model, PCM.

The two planar conformations ($\tau=0^\circ$ and $\tau=180^\circ$) were fully optimised and the minima being checked by calculating the vibrational frequencies. The calculations for the other conformers were done maintaining the τ value constant and allowing the relaxation of all the other internal coordinates. The TDDFT calculations were carried out at the previously optimised geometry.

RESULTS AND DISCUSSION

Although 2-acetylphenoxathiin-sulphone is an achiral compound, in the presence of increasing concentrations of CyDs, a dichroic spectrum appears in the region of its absorption electronic spectrum, 250-310 nm, in a different region from the bands of the CyDs, located in the far UV, around 180 nm. As a confusion or overlap of the signals is ruled out, these signals were assigned to the induced dichroism of the ligand, determined by an asymmetry in the local environment occurring upon the inclusion process. An example is given for β -CyD in Fig. 2. At gradual increase of β -CyD, two positive bands at 280 nm and 259-262 nm are apparent, this last one being more intense. Dichroic bands were obtained for all the three CyDs used, but the main aspects of the bands were somewhat different, likely reflecting the effect of the cavity dimensions.

The ICD spectra recorded for similar concentrations of the three CyDs are presented in Fig. 3. It can be seen that in the presence of 2HP- β -CyD, the ICD spectrum is characterized by the two positive bands, as previously discussed for β -CyD. However, at the same concentration of CyDs, the relative intensities of these two bands are different. In the presence of 2HP- β -CyD only the band at 261 nm has a significant intensity, the other band being observed merely as a shoulder. In the same time, a very low intensity signal is evidenced around 300 nm. A deconvolution of the ICD spectrum (Fig. 3, inset) leads to the exact positions of the three bands at 260 nm, 284 nm and 309 nm.

In the case of α -CyD, both main ICD bands are evidenced but with a negative sign, and different relative intensities, the band at 285 nm being the most intense. Comparing the intensities of the bands in this CyD with the previous ones, lower CD values can be seen, *i.e.* a less ICD effect, reflecting a lower interaction or a different kind of complex.

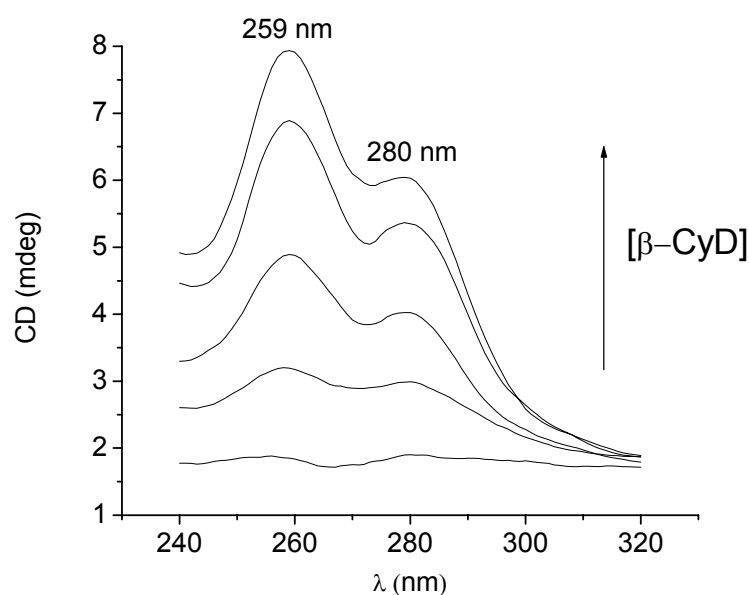


Fig. 2 – Induced circular dichroism spectra of **I** in the presence of increasing concentrations of β -CyD.

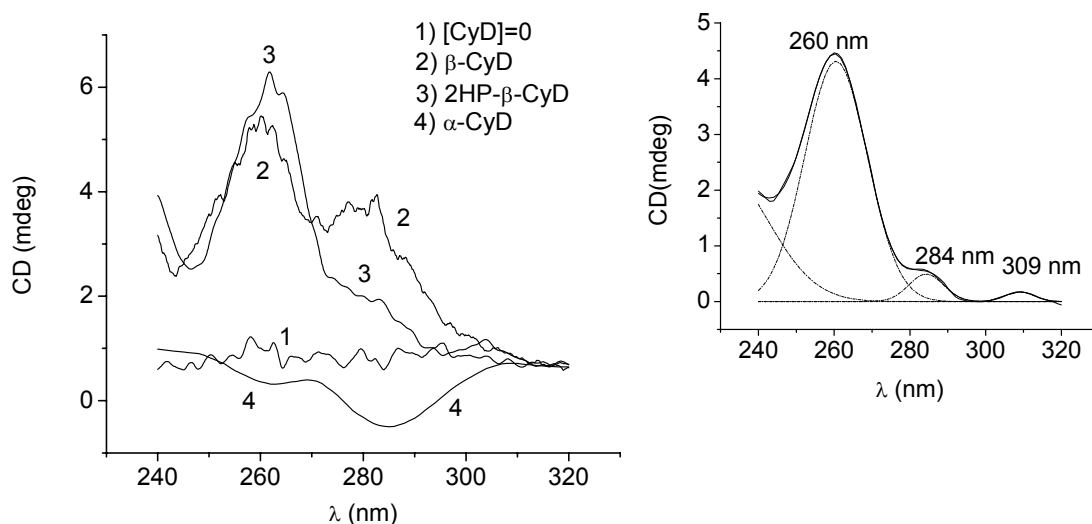


Fig. 3 – Induced circular dichroism bands of **I** in the absence (1) and in the presence of equal concentrations of CyDs (2, 3, 4). Inset: deconvolution of the smoothed ICD spectrum recorded in the presence of 2HP- β -CyD.

The binding constants for the complexes with β - and 2HP- β -CyD, K , were estimated using linear and nonlinear regression models³⁸⁻⁴⁴ for a complex with 1:1 stoichiometry, in terms of $\Delta\theta$, the difference between experimental ellipticities of the guest in the absence and presence of CyD read at a definite wavelength and the total molar concentrations of the guest and the cyclodextrins, $[G]$ and $[CyD]$, respectively.

The linear model is based on eq. (1) known as the Scott³⁸ equation:

$$\frac{[G][CyD]d}{\Delta\theta} = \frac{[CyD]}{\Delta\psi} + \frac{1}{K\Delta\psi} \quad (1)$$

where $\Delta\psi$ represents the difference in the molar ellipticity coefficient between the complexed and free guest and d is the path-length of the cell.

The non linear model corresponds to eq. (2)

$$\Delta\theta = \frac{k}{2} \left([CyD] + [G] + K^{-1} - \sqrt{([CyD] + [G] + K^{-1})^2 - 4 \times [CyD] \times [I]} \right) \quad (2)$$

where $\Delta\theta$ and K have the same meaning as in eq. (1) and k is correlated with the dichroic signal at total complexation.

The experimental readings at the most intense dichroic wavelengths for each CyD, 280 nm for β -

CyD and 261 nm for 2HP- β -CyD, are plotted vs. the ligand concentrations in Figs. 4 and 5. The curves represent the best fit to the aforementioned equations and the resulted binding constants are listed in Table 1.

Table 1

Association constants, K (M^{-1}), obtained by fitting the experimental data to eqs. (1) and (2) and r the correlation coefficient of the fit

CyD	β -CyD		2HP- β -CyD	
Model	Eq. 1	Eq. 2	Eq. 1	Eq. 2
K	276.2	260.4	588.1	569.3
r	0.976	0.986	0.972	0.977

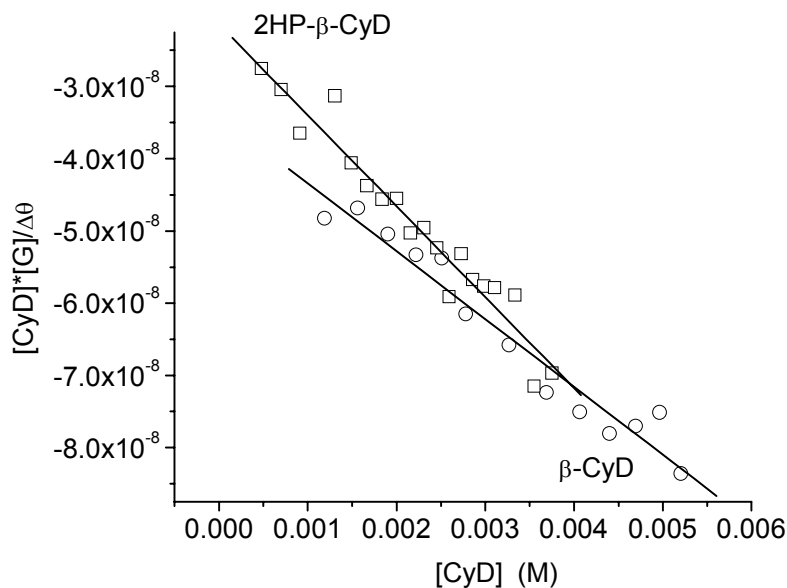


Fig. 4 – Determination of the association constants using a linear regression model. The ellipticities were read at 280 nm for β -CyD and 261 nm for 2HP- β -CyD. The lines represent the best fit to eq. (1) yielding the constants listed in Table 1.

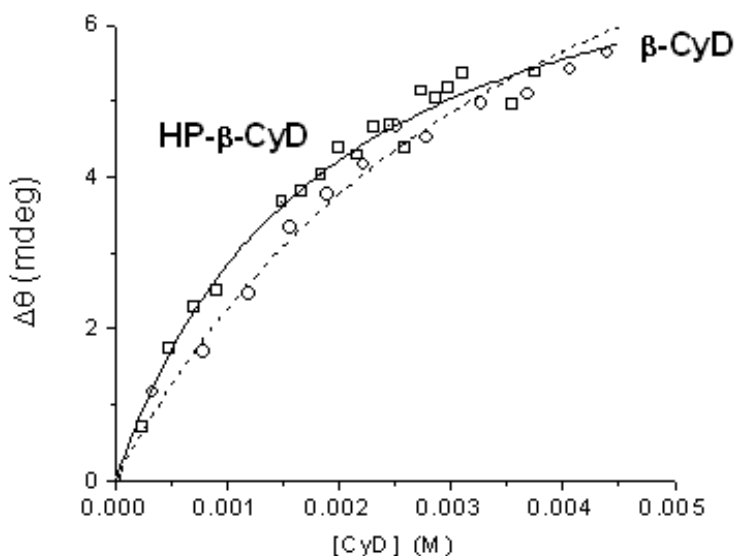


Fig. 5 – Determination of the association constants using a nonlinear regression model. The ellipticities were read at 280 nm for β -CyD and 261 nm for 2HP- β -CyD. The curves represent the best fits to eq.(2) yielding the constants listed in Table 1.

The binding constant for the inclusion complex in α -CyD was not estimated due to the low variation in the ellipticities with the CyD concentration and the uncertainty in the complex stoichiometry.

According to the already mentioned semiempirical Harata-Kodaka rules for the inclusion of the guest in the CyD cavity, several assumptions can be made concerning the position of the ligand in the cavity. The presence of positive bands in the ICD spectra of the β -CyD and 2HP- β -CyD complexes attests a quasi-parallel direction of the associated transition moments with the cavity axis. The change in the sign of the dichroic bands in the inclusion complex with α -CyD reflects a different position of the molecule, presumably an orthogonal one in respect to the long cavity axis. The lower dimension of this CyD as compared to the other two forces the ligand to adopt a different inclusion mode or in some cases favors the formation of a 1:2 ligand:cyclodextrin complex.⁴⁵

The DFT and TDDFT calculations were performed to have an insight on the positions of the absorption bands and the polarizations of the corresponding transitions, in order to get theoretical support for our experimental data. According to literature reports,^{46,47} one of the problems in explaining the ICD spectra is to find the structural element that can be correlated with

the appearance of the molecular asymmetry, when the molecule is confined in a restricted position. In the interaction of some ligands with human and bovine serum albumins it was considered as a possible asymmetry source the change in the position of the substituent (COOH, substituted phenyl group, *etc.*) in respect with the planar system of the chromophore. In our case, we have assumed that the asymmetry occurs due to the change in the acetyl position in respect with the heteroring, described by the torsion angle τ .

Therefore, the electronic transitions were calculated for several conformers characterized by different τ values. τ was varied with a step of 30° in the range of $0^\circ - 180^\circ$. The experimental spectrum and the calculated ones for the planar, $\tau = 0^\circ$, and twisted, $\tau = 90^\circ$, conformers are displayed in Fig. 6.

Some relevant results are listed in Tables 2 and 3 and the directions of the transitions moments for the most intense ($f > 0.0030$) electronic bands in the range 230-350 nm are displayed in Fig. 7 for three conformers ($\tau: 0^\circ; 60^\circ; 90^\circ$).

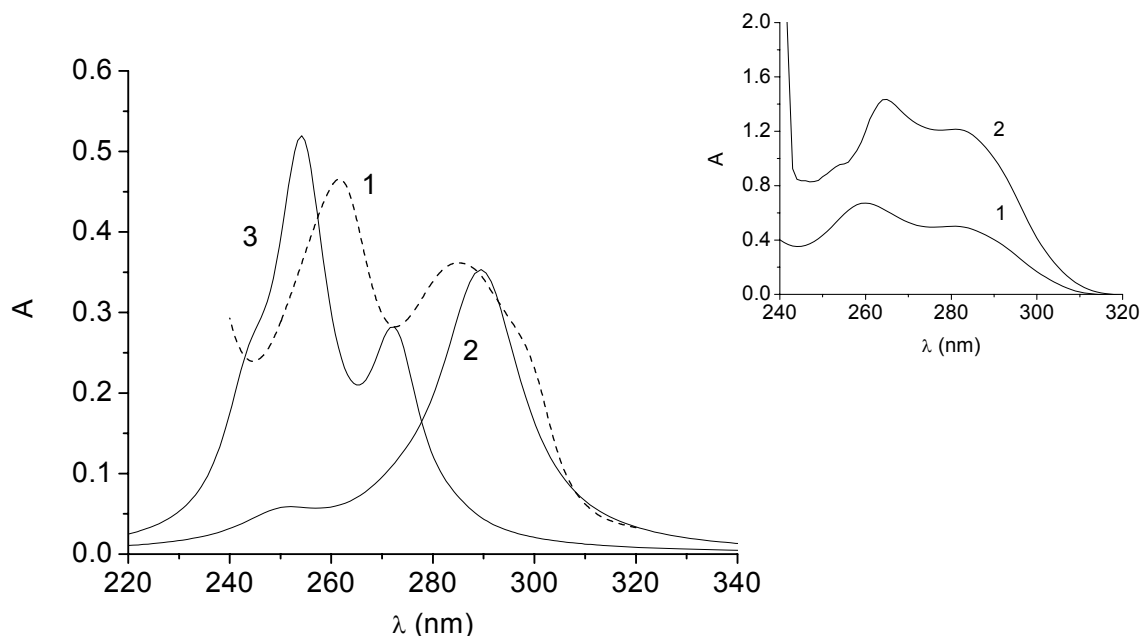


Fig. 6 – Experimental and calculated TDDFT (B3LYP/6-31G) absorption spectra of **I**: 1) experimental; 2) calculated, $\tau = 0^\circ$; 3) calculated, $\tau = 90^\circ$. Inset: experimental spectra in methanol (1) and ethylene glycol (2).

Table 2

Wavelengths (λ), oscillator strengths (f) and assignment ($h = \text{homo}$; $l = \text{lumo}$) of the electronic absorption bands calculated at the B3LYP/6-31G level for the totally planar, $\tau=0^\circ$ and 180° and twisted conformers, $\tau=90^\circ$

$0^\circ; 180^\circ$				90°			
τ				τ			
E	-1238.5291566 Ha ; -1238.5294281Ha			E	-1238.51806 Ha		
Nr	λ (nm)	f	Assignment	Nr	λ (nm)	f	Assignment
1	324.99	0.0002	$h-l \rightarrow l$	1	286.43	0.0021	$h-l \rightarrow l+2$
2	289.51	0.3448	$h \rightarrow l$	2	273.57	0.0569	$h \rightarrow l$
3	273.63	0.0230	$h \rightarrow l+1$	3	255.55	0.1169	$h \rightarrow l+1$
4	250.07	0.0332	*	4	244.37	0.0310	$h-l \rightarrow l$

*Contribution of more than two transitions.

Table 3

Wavelengths (λ) and oscillator strengths (f) of the electronic absorption bands calculated at the B3LYP/6-31G level for some intermediate values of τ

τ	30°		60°		120°		150°	
E	-1238.5271036 Ha		-1238.519745 Ha		-1238.522454 Ha		-1238.5274263 Ha	
Nr	λ (nm)	f	λ (nm)	f	λ (nm)	f	λ (nm)	f
1	316.40	0.0035	297.12	0.0101	298.51	0.0239	317.32	0.0135
2	283.29	0.3180	273.39	0.0492	274.83	0.0491	284.31	0.3084
3	273.15	0.0363	267.88	0.2412	268.94	0.2387	274.64	0.0373
4	248.76	0.0417	247.75	0.0548	248.05	0.0133	249.23	0.0185

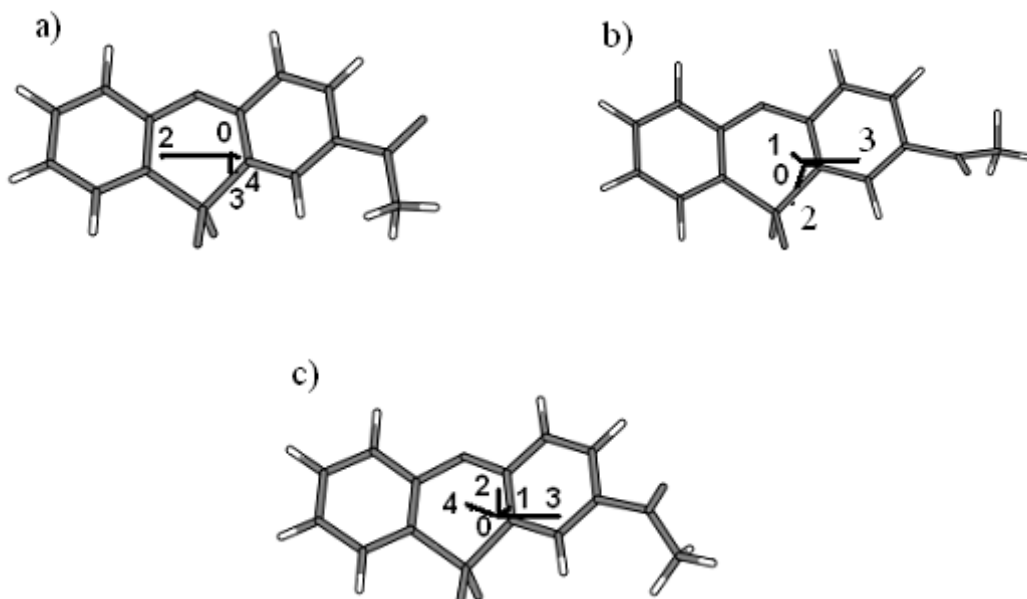


Fig. 7 – Directions of the relevant transition moments ($f > 0.0030$) for the bands in the range of 230-350 nm: a) $\tau = 0^\circ$; b) $\tau = 90^\circ$ c) $\tau = 60^\circ$. 0 represents the origin of the molecular axes, and the numbers correspond to the transitions in Table 2.

A first check of the theoretical results was made by comparing the calculated UV spectrum with the experimental spectrum in the absence of the CyDs. The experimental electronic spectrum of 2-acetylphenoxathiin-sulphone in water, in the range 240-350 nm consists of three bands located at 261, 286 and 300 nm. The last two bands are overlapped and of different intensities, the band at 300 nm being characterized by the lowest extinction coefficient and its maximum was obtained after a

deconvolution of the spectrum. The comparison of the spectra in Fig. 6 leads to the following observations. Although the predicted positions of the bands correspond in a satisfactory manner with the experimental spectrum, this one is wider than the calculated spectra, presumably reflecting the presence in solution of different conformers.

The DFT calculations predict as more stable the planar conformations. An estimation of the barrier to rotation considering the difference between the

energy for $\tau = 90^\circ$ (maximum point on the potential energy surface built in respect to the torsion angle τ) and the energy for the minimum planar conformation ($\tau = 180^\circ$), the values are 6.93 kcal/mol and 6.42 kcal/mol for the B3LYP and PBE functionals, respectively. Although these barriers are overestimated, the values are not too high as to rule out the presence of other conformers. Theoretically, it is not possible to make a convolution of the spectra for the different conformers, as the exact population of each one is difficult to estimate. However, the possible presence of several conformers was experimentally checked by recording the absorption spectrum in ethylene glycol, known for its larger viscosity as compared to methanol or water (inset of Fig. 6). The observed changes in the position and relative intensities of the bands can be explained by the reduced possibility of internal rotation in this solvent, favouring some conformers, *i.e.* a different conformer population as in methanol.

Analysing the results for the two limit conformers, the planar and the twisted one (Table 2), it can be seen that the calculated spectra differ by the positions and the relative intensities of the bands. The calculations for the planar conformers account well for the intense band at 280 nm,

whereas the calculated spectrum for the twisted conformer corresponds better to the second part of the experimental spectrum, the region around 262 nm. At $\tau = 90^\circ$, the twisting of the substituent determines a decrease in the extent of the overall conjugation as compared to the case of planar conformers and, therefore, the band positions are shifted towards lower wavelengths. As concern the relative intensities of the bands, for both planar conformers ($\tau = 0^\circ$ and $\tau = 180^\circ$) the most intense is the longest wavelength band at 292 nm, while for the twisted conformation the intensities are reversed, the band at 250 nm being the most intense.

The calculations performed using the other functional, PBE, predict generally the same effects, but the positions of the bands are hypsochromically shifted. However, apart from this shift of the entire spectrum, we can consider the calculations reliable enough for the discussion of the experimental ICD results in terms of the polarizations of the electronic transitions.

The theoretical results for the two planar conformers are quite similar as concerns the positions, the oscillator strengths and the assignment of the bands and therefore Table 2 refers to $\tau=0^\circ$ conformer.

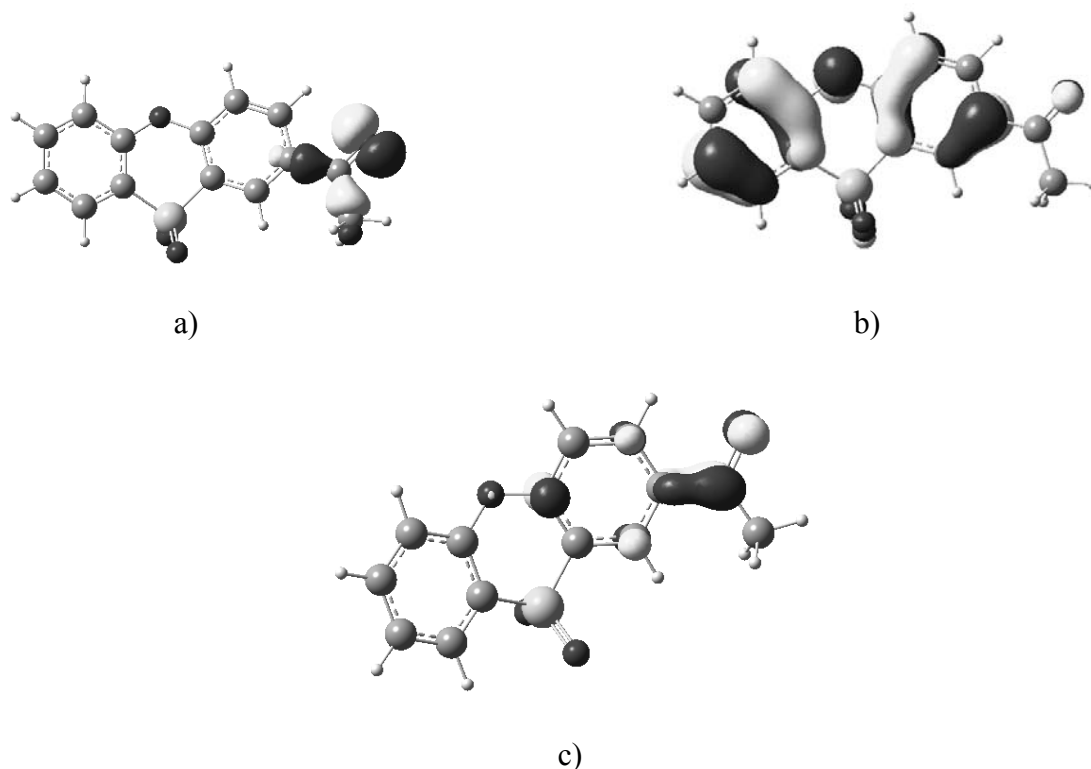


Fig. 8 – Molecular orbitals implied in the electronic transitions, calculated for the planar conformation, $\tau = 0^\circ$: a) *homo-1*; b) *homo*; c) *lumo*.

The band at 289.51 nm, the most intense, is assigned to the *homo-lumo* transition and the transition moment is polarized along the x axis, the long axis of the molecule in our coordinate system. Inspection of the molecular orbitals (Fig. 8) shows that for the planar conformers, both frontier orbitals are π orbitals, *homo* being mainly localized on the whole phenoxathiin ring and the carbonyl group of acetyl and *lumo* only on the acetyl-substituted ring and the C=O group. *Homo-1* is localized only on the acetyl group and corresponds to the *n* orbital of the oxygen. The significant contribution of the acetyl group to the frontier orbitals explains the dependence of the *homo-lumo* transition on the acetyl position, the shift of the maximum from 289.51 nm to 273.57 nm and the decrease of the oscillator strength from 0.3448 to 0.0569 for $\tau = 90^\circ$ as compared to the planar conformers. For the nonplanar conformations (intermediate values of τ), the functions of the excited states do no more correspond to a single electronic transition and contain contributions of several excitations. Therefore, the assignment is no more given in Table 3. Inspection of Fig. 7 shows that for the planar conformer, the moment corresponding to transitions 2 and 4 (289.51 nm and 257 nm) are polarized along the long molecular axis and transition 3 is polarized along the short molecular axis. As transition 2 is significantly the most intense, $f = 0.3448$ as compared to f about 0.03 for transitions 3 and 4, it is expected that for this conformer, the general behavior in the presence of CyD should be determined by transition 2. For the twisted $\tau = 90^\circ$ conformation, the most intense transition is 3, $\lambda = 255.55$ nm, $f = 0.1158$, and its moment is directed along the long molecular axis.

A comparison of the experimental ICD spectrum in the presence of β -CyD with the calculated electronic transitions for these two conformers shows that a parallel (axial) mode of inclusion is accounted for by the calculations. For these conformations the most intense transitions (2 for $\tau = 0^\circ$; 3 for $\tau = 90^\circ$) are polarized along the long molecular axis and their positions are in good agreement with the experimental bands. It is however difficult to make a prediction on the most favoured conformers, but the high intensity of the positive dichroic signal at 280 nm suggests a predominance of the quasi-planar conformers.

As was previously discussed, the main differences between the ICD spectrum in 2HP- β -CyD as compared to β -CyD are the significant

decrease of the intensity of the band at 289.5 nm and the appearance of the low positive band at 300 nm. The values of the oscillator strengths for $\tau = 60^\circ$ explain the change of the band intensities in the ICD spectrum as compared to that in β -CyD. Using the B3LYP functional, for $\tau = 60^\circ$, the most intense band is shifted from $\lambda = 289.5$ nm for the planar conformers to 268 nm, the transition remaining polarized along the x axis, *i.e.* parallel to the cavity axis. In the same case the longest wavelength band predicted at 297 nm and practically not observed in the case of β -CyD, shows an increase in the f value explaining its evidence in this case. We suggest therefore that the cavity of 2HP- β -CyD allows an axial inclusion mode, but determines also a selection of the included conformers, the conformers with τ around 60° being favoured.

In the case of α -CyD, the same ICD bands are observed but the sign is negative. We can therefore assume an orthogonal position of the guest in respect with the cavity axis; that corresponds better to a 1:2 ligand: α -CyD stoichiometry.

CONCLUSIONS

The present results lead to the following conclusions. The binding constants of the cyclodextrin inclusion complexes of an achiral compound can be estimated with sufficient reliability using the experimental ICD data of the ligands for the cases in which the induced ellipticities are large enough, up to 8-10 mdeg. In the present case, this was possible for β - and 2HP- β -CyD, which form 1:1 complexes with **I**, but not for α -CyD. The binding constant for the system **I** - β -CyD is in good agreement with that obtained by fluorescence measurements (manuscript in preparation). The correlation of the Harata and Kodaka empirical rules with TDDFT calculations provide a rational explanation for the differences between the induced signals in the β -CyD and 2HP- β -CyD, considering that the asymmetry produced by the inclusion process is represented by the torsion of the acetyl group in respect with the π system of the heteroaromatic ring and by the preferential inclusion of different conformers, dependent on the cavity dimension. In the case of α -CyD, both the experimental and theoretical results support the formation of a complex with 1:2 ligand:cyclodextrin stoichiometry. As a general

conclusion, we can say that the correlation of the ICD results with TDDFT data on the polarisations of the electronic transitions can be used for obtaining good starting geometry for the optimisations of the supramolecular ligand: cyclodextrin complexes.

Acknowledgement: Thanks are due to Dr. P. Filip, "C. D. Nenitescu" Institute of Organic Chemistry of the Roumanian Academy for allowing the calculations with the Gaussian program.

REFERENCES

1. K.H. Fromming, "Cyclodextrins in Pharmacy", Kluwer Academic Publishers, 1994.
2. R. Stancanelli, A. Mazzaglia, S. Tommasini, M.L. Calabro, V. Villari, M. Guardo, P. Ficarra and R. Ficarra, *J. Pharm. Biomed. Anal.*, **2007**, *44*, 980-984.
3. H. Loftsson and D. Duchêne, *Int. J. Pharm.*, **2007**, *329*, 1-11.
4. Y. Nagas, M. Hirata, K. Wada, H. Arima, F. Hirayama, T. Irie, M. Kikuchi and K. Uekama, *Int. J. Pharm.*, **2001**, *229*, 163-172.
5. E. M. Martin Del Valle, *Process Biochem.*, **2004**, *39*, 1033-1046.
6. J. Szejtli, "Cyclodextrin Technology", Kluwer Academic Publishers, Dordrecht, 1988.
7. J. Szelti, *Chem. Rev.*, **1998**, *98*, 1743-1754.
8. H. Dodziuk, "Cyclodextrins and Their Complexes Chemistry, Analytical Methods, Applications", Wiley-VCH, 2006.
9. F. Mendicuti and M. Jose Gonzalez-Alvarez, *J. Chem. Educ.*, **2010**, *87*, 965-968.
10. M. Oana, A. Tintaru, D. Gavrilu, O. Major and M. Hillebrand, *J. Phys. Chem. B*, **2002**, *106*, 257-263.
11. A. Tintaru, M. Hillebrand and A. Thevand, *J. Incl. Phen. Macrocycl. Chem.*, **2003**, *45*, 35-40.
12. I.V. Muthu, V. Enoch and M. Swaminathan, *J. Incl. Phenom. Macrocycl. Chem.*, **2005**, *53*, 149-154.
13. M. Sowmiya, P. Purkayastha, A.K. Tiwari, S.S. Jaffer and S.K. Saha, *J. Photochem. Photobiol. A: Chem.*, **2009**, *205*, 186-196.
14. H.J. Schneider, F.Hacket, V. Rüdiger and H. Ikeda, *Chem. Rev.*, **1998**, *98*, 1755-1786.
15. M. Zhang, J. Li, Li. Zhang and J. Chao, *Spectrochim. Acta A*, **2009**, *71*, 1891-1895.
16. N. Berova and K. Nakanishi, "Circular Dichroism, Principles and Applications", 2nd edition, N. Berova and K. Nakanishi, R. W. Woody (Eds.), Wiley-VCH, New York, 2000, p. 337-382.
17. S. Allenmark, *Chirality*, **2003**, *15*, 409-422.
18. G. Marconi, S. Monti, B. Mayer and G. Kohler, *J. Phys. Chem.*, **1995**, *99*, 3943-3950.
19. S. Monti, F. Manoli, I. Manet, G. Marconi, B. Mayer, R.E. Tormos and M.A. Miranda, *J. Photochem. Photobiol. A: Chemistry*, **2005**, *173*, 349-357.
20. P. Fini, L. Catucci, M. Castagnolo, P. Cosma, V. Pluchinotta and A. Agostiano, *J. Incl. Phenom. Mol.*, **2007**, *57*, 663-668.
21. M.D. Veiga, M. Merino, M. Cirri, F. Maestrelli and P. Mura, *J. Incl. Phenom.*, **2005**, *53*, 77-83.
22. G. Marconi, S. Monti, F. Manoli and S. Ottani, *J. Incl. Phenom. Macrocycl. Chem.*, **2007**, *57*, 279-282.
23. G. Marconi, S. Monti, F. Manoli, Alessandra Degli Esposti and B. Mayer, *Chem. Phys. Lett.*, **2004**, *383*, 566-571.
24. I. Matei, L. Soare, C. Tablet and M.Hillebrand, *Rev. Roum. Chim.*, **2009**, *54*, 133-141.
25. A. Banerjee, K. Basu and P.K. Sengupta, *J. Photochem. Photobiol. B: Biology*, **2007**, *89*, 88-97.
26. Z. Lu, C. Lu and Q. Meng, *J. Incl. Phenom. Macrocycl. Chem.*, **2008**, *61*, 101-106.
27. K. Harata and H. Uedaira, *Bull. Chem. Soc. Japan*, **1975**, *48*, 375-378.
28. H. Shimidzu, A. Kaito and M. Katano, *Bull. Chem. Soc. Japan*, **1979**, *52*, 2678-2684.
29. M. Kodaka and T. Fukaya, *Bull. Chem. Soc. Jap.*, **1989**, *62*, 1154-1157.
30. M. Kodaka, *J. Phys. Chem.*, **1991**, *95*, 2110-2119.
31. M. Kodaka, *J. Am. Chem. Soc.*, **1993**, *115*, 3702-3705.
32. M. Kodaka, *J. Phys. Chem. A*, **1998**, *102*, 8101-8103.
33. GAUSSIAN03: General Atomic and Molecular Electronic Structure System M.W.Schmidt, K.K. Baldrige, J.A. Boatz, S.T. Elbert, M.S. Gordon, J.H. Jensen, S. Koseki, N. Matsunaga, K.A. Nguyen, S. Su, T.L. Windus, M. Dupuis, J.A. Montgomery J. Comput. Chem. *14* (1993) 1347-1363; M.S. Gordon, M.W. Schmidt, in: C.E. Dykstra, G. Frenking, K.S. Kim, G.E. Scuseria (Eds.), *Theory and Applications of Computational Chemistry: the first forty years*, Elsevier, Amsterdam, 2005, p. 1167-1189.
34. A.D. Becke, *J. Chem. Phys.*, **1993**, *98*, 5648-5652.
35. B. Miehlich, A. Savin, H. Stoll and H. Preuss, *Chem. Phys. Lett.*, **1989**, *157*, 200-206.
36. P. Perdew, K. Burke and Y. Wang, *Phys. Rev. B*, **1996**, *54*, 16533-16539.
37. J.P. Perdew, K. Burke and M. Ernzerhof, *Phys. Rev. Lett.*, **1996**, *77*, 3865-3868.
38. R.L. Scott, *Rec. Trav. Chim.*, **1956**, *75*, 787.
39. F. Barbato, B. Cappello, M.I. La Rotonda, A. Miro and F. Quaglia, *J. Incl. Phenom. Macrocycl. Chem.*, **2003**, *46*, 179-185.
40. F. Zsila, Z. Bikadi and M. Simonyi, *Biochem. Pharmacol.*, **2003**, *65*, 447-456.
41. Y. Liu, B. Li, T. Wada and Y. Inoue, *Tetrahedron*, **2001**, *57*, 7153-7161.
42. Y. Takenaka, H. Nakashima and N. Yoshida, *J. Mol. Struct.*, **2007**, *871*, 149-155.
43. F. Zsila, Z. Bikadi and S.F. Lockwood, *Bioorg. Med. Chem. Lett.*, **2005**, *15*, 3725-3731.
44. J.W. Park, H.E. Song and S.Y. Lee, *J. Phys. Chem B*, **2002**, *106*, 7186-7192.
45. S. Hamai, *J. Inclusion Phenom. Mol.*, **1997**, *27*, 57-67.
46. F. Zsila, Z. Bikadi, I. Fitos and M. Simonyi, *Curr. Drug Discov. Technol.* **2004**, *1*, 133-153.
47. F. Zsila, T. Imre, P.T. Szabó, Z. Bikadi and M. Simonyi, *FEBS Lett.*, **2002**, *520*, 81-87.

